# Traveling wave states in pipe flow

S. Tanveer
Collaborators: O.Ozcakir, P.Hall, E.Overman

May 23, 2016

# Pipe Flow: Description

Navier-Stokes equations has a well-known simple solution in an infinitely long cylindrical pipe; in non-dimensional form, velocity is given by:

$$\vec{v}_P(r) = (1 - r^2)\widehat{\boldsymbol{z}} \quad \text{with} \quad \nabla p = -\frac{4}{R}\widehat{\boldsymbol{z}}$$

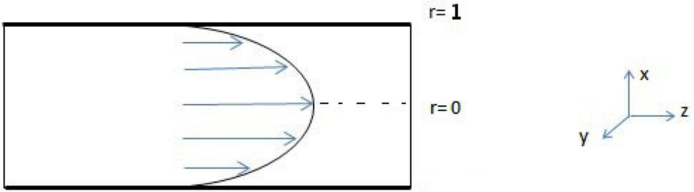


- Evidence also suggests that this flow is linear stable for all $R$.

Reynolds explored the behaviour of flow in a long pipe for different $R$.

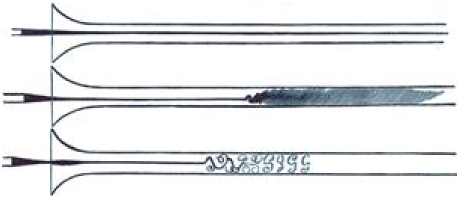

Ink was injected centerline of a pipe carrying water and he observed

- For $R < R_{c,1}$, any perturbation eventually decays in time
- For $R > R_{c_2} > R_{c,1}$ the Hagen-Poiseuille flow becomes irregular, and exhibits complex spacetime behaviour

- For $R_{c,1} < R < R_{c,2}$, the behavior seemed to depend on amplitude of disturbance

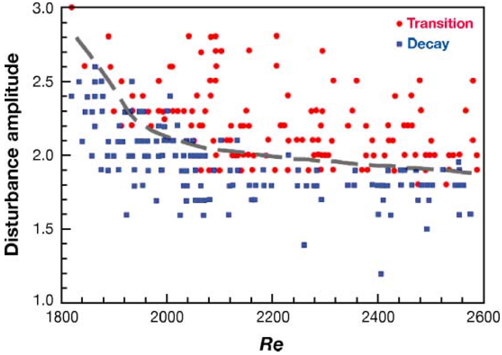


Darbyshire & Mullin did a systematic study on disturbance amplitude effect.

The observed instability threshold in their experiment decreased with increasing $R$.

If we decompose $\vec{v} = \vec{v}_B + \boldsymbol{v}$, where $\vec{v}_B$ is a steady base flow ($\vec{v}_B \neq \vec{v}_P$ when suction-injection is applied at the walls), then $\boldsymbol{v}$ satisfies

$$\frac{\partial \boldsymbol{v}}{\partial t} = -(\boldsymbol{v} \cdot \nabla)\boldsymbol{v} - \nabla q + \frac{1}{R}\Delta \boldsymbol{v} - (\vec{v}_B \cdot \nabla)\boldsymbol{v} - (\boldsymbol{v} \cdot \nabla)\vec{v}_B$$
$$\nabla \cdot \boldsymbol{v} = 0 \ \text{ with } \ \boldsymbol{v}(1, \theta, z, t) = 0 \ \text{ at the wall in cylindrical coords.}$$

Abstractly, we may write

$$\frac{d\vec{X}}{dt} = f(\vec{X}; \vec{\beta})$$

$\vec{X}$=representation of a perturbed velocity field $\boldsymbol{v}$ in the space of solenoidal vector field, $\vec{\beta} = (R, \alpha)$ are parameters of the system.

# Relevant questions for the dynamical system

- Existence of Steady states solutions.
- Existence of traveling wave/time periodic solutions.
- Dynamical behavior of trajectories in phase-space.

cartoon of phase-space portrait (Duguet *et. al. '08a*

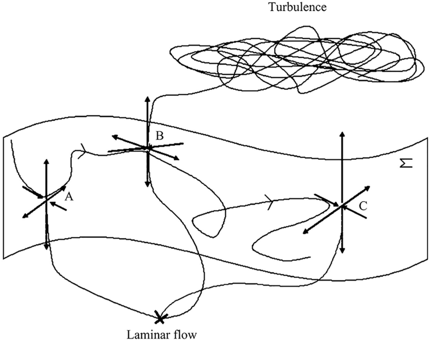


Evidence suggests boundary Σ of basin of attraction contains TW states.

# Pipe flow transition: Traveling Waves

A traveling wave, which are also time periodic solutions in the lab frame, is of the form

$$\boldsymbol{v} = \sum_{k,l \in \mathbb{Z}^2} \vec{v}_{kl}(r) e^{ikk_0\theta} e^{il\alpha(z-ct)}$$

Lumping separately $l = 0$ and $l \neq 0$ terms, we may write

$$\boldsymbol{v} = \underbrace{\begin{pmatrix} U(r,\theta) \\ V(r,\theta) \\ 0 \end{pmatrix}}_{\text{rolls}} + \underbrace{\begin{pmatrix} 0 \\ 0 \\ W(r,\theta) \end{pmatrix}}_{\text{streaks}} + \underbrace{\begin{pmatrix} \hat{u}(r,\theta,z-ct) \\ \hat{v}(r,\theta,z-ct) \\ \hat{w}(r,\theta,z-ct) \end{pmatrix}}_{\text{waves}}$$

where z-averaged $\langle \widehat{\boldsymbol{u}} \rangle = \langle (\widehat{u}, \widehat{v}, \widehat{w}) \rangle = \vec{0}$, $\mathbf{U} = (U, V, W)$.
Existence of such states may be understood physically as a self sustaining three-way interaction between rolls, streaks and waves.

This nonlinear three-dimensional process, sometimes referred to as *Self-Sustaining Process(SSP)*, is a generic mechanism in shear flows. First proposed by Benney, developed further by Smith and Hall and applied systematically to a Plane-Couette flow by Waleffe and extended by others.

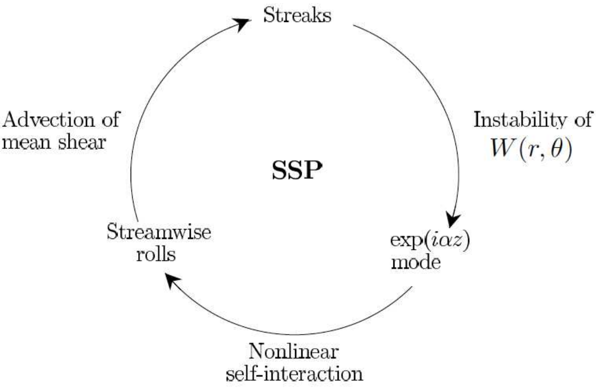


Self Sustaining Process Diagram (Waleffe '97)

Figure shows how rolls affect streamwise velocity to create streak instability. Streamwise rolls $(U, V)$ act as forcing in the $z$ direction.

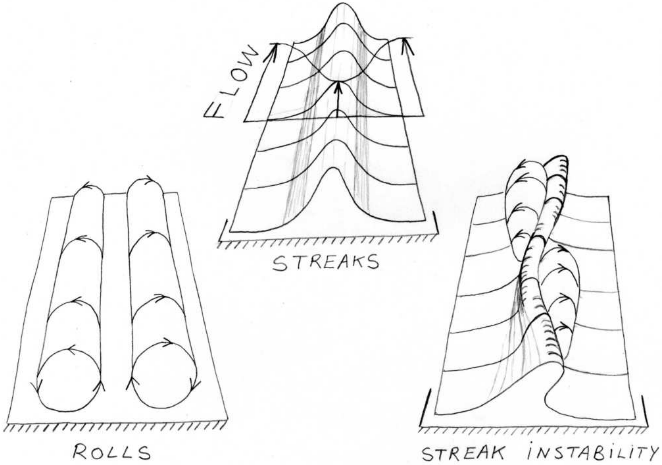


Streak Instability Cartoon in Plane-Couette Flow. 'Rolls' and 'Streaks' (Waleffe '06)

- Numerical calculation of these states requires good initial guess for Newton iteration to converge.
- Other authors tried adhoc approach towards suitable initial guess (eg. Wedin &Kerswell '04).
- Note that these states cannot be obtained through a continuation of Hagen-Poiseuille flow since it has no finite $R$ bifurcation point.

## Our Methodology

- Since small rolls induces large streaks, we perturbed the base flow through azimuthal suction/injection at the walls and obtained a flow with a finite critical $R$ for linear instability.
- The Hopf-Bifurcation at critical $R$ provides a good initial guess for TW states with suction/injection, which is switched off far from bifurcation point.

# Base Flow with suction-injection

Through numerical continuation in suction-injection parameter $s$, we calculate base flow $\vec{v}_B(r,\theta)$ which satisfies Navier-Stokes with $\vec{v} = \vec{v}_{wall}(\theta; s)$ on $r = 1$ where

$$\vec{v}_{wall}(\theta; s) = \frac{s}{R}\cos(k_0\theta)\widehat{\boldsymbol{r}}.$$

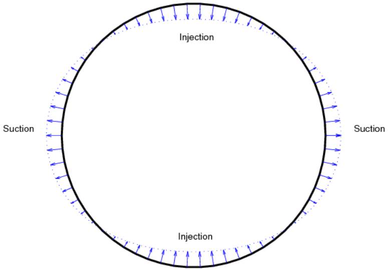


Alternate suction/injection imposed at $r = 1$ when $k_0 = 2$

# Computation Steps

- $\vec{v}_B$ for $s > 0$ is determined to be neutrally stable at some $\alpha$ at some large but finite $R$.
- We compute neutrally stable modes $\widehat{\boldsymbol{u}}$
- TW computed with initial guess $\boldsymbol{v}_0 = \widehat{\varepsilon}_0 \widehat{\boldsymbol{u}}$ in a Newton iteration process to find $\vec{v}$.

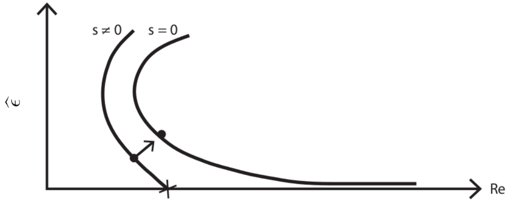


Bifurcation point changes to finite $R$ shown by $\times$ when $s \neq 0$.

The TW states obtained in this manner sustains itself without suction-injection ($s \to 0$) when sufficiently far from the Hopf-bifurcation

# Numerical solution

Solutions with Rotational symmetric $R_{k_0}$, at the truncation $(N, M, P)$ in the form

$$\boldsymbol{v} = \sum_{\substack{l \text{ even} \\ j=0,\dots,N \\ k=0,\dots,M}} \begin{pmatrix} (u^1_{jkl}\cos l\tilde{z} + u^2_{jkl}\sin l\tilde{z})\Phi_j(r;kk_0)\cos kk_0\theta \\ (v^1_{jkl}\cos l\tilde{z} + v^2_{jkl}\sin l\tilde{z})\Phi_j(r;kk_0)\sin kk_0\theta \\ (w^1_{jkl}\sin l\tilde{z} + w^2_{jkl}\cos l\tilde{z})\Psi_j(r;kk_0)\cos kk_0\theta \end{pmatrix}$$

$$+ \sum_{\substack{l \text{ odd} \\ j=0,\dots,N \\ k=0,\dots,M}} \begin{pmatrix} (u^1_{jkl}\cos l\tilde{z} + u^2_{jkl}\sin l\tilde{z})\Phi_j(r;kk_0)\sin kk_0\theta \\ (v^1_{jkl}\cos l\tilde{z} + v^2_{jkl}\sin l\tilde{z})\Phi_j(r;kk_0)\cos kk_0\theta \\ (w^1_{jkl}\sin l\tilde{z} + w^2_{jkl}\cos l\tilde{z})\Psi_j(r;kk_0)\sin kk_0\theta \end{pmatrix}.$$

are found, where $\tilde{z} = \alpha(z - ct)$, with certain choice of $\Phi_j(r), \Psi_j(r)$, and using $S$ (shift-rotate) and $S_1$ (shift-reflect) symmetries.

# Results

We restricted our calculations to ($S$-symmetric) $R_2-$ solutions

- Reproduced the solution of Wedin & Kerswell (2004) for $k_0 = 2$.
- Two new TWs found: $C1$ and $C2$ calculated for upto $R = 2 \times 10^5$.
- In the light of numerical evidence; we also explored $R \to \infty$ asymptotics of TW states.

# Roll and Streak profiles at $R = 10^4$ for $\alpha = 1.55$.

(a) $C1$ (b) $C2$

- Besides the $S$-symmetry (shift-and-reflect) the $C2$ branch also has $\Omega_2$-symmetry (shift-and-rotate) (Pringle et. al. (2009))

(c) $WK$

(d) $WK2$

# Roll and Streak profiles at $R = 10^5$ for $\alpha = 1.55$.

(e) $C1$ (f) $C2$ (g) $WK$

- shrinking core structure observed for $C1, C2$.

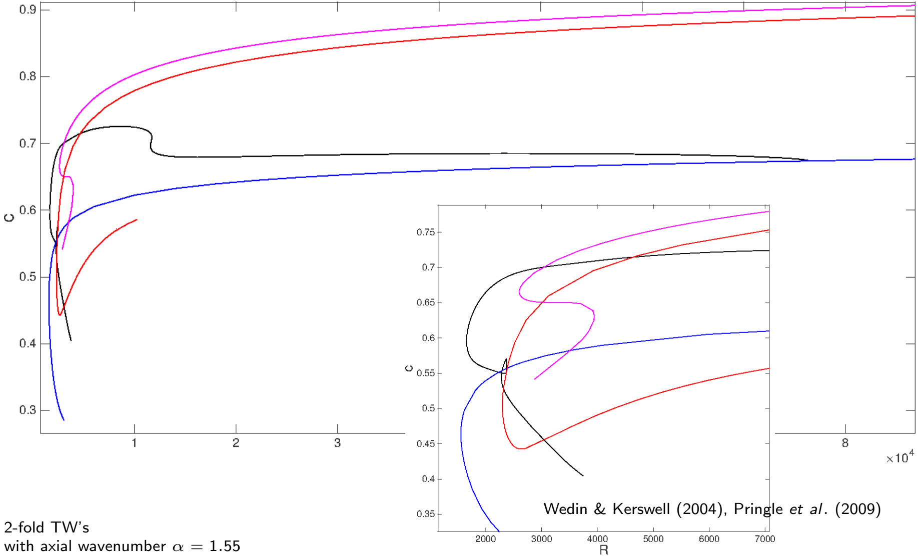


Wedin & Kerswell (2004), Pringle *et al*. (2009)

2-fold TW's
with axial wavenumber $\alpha = 1.55$

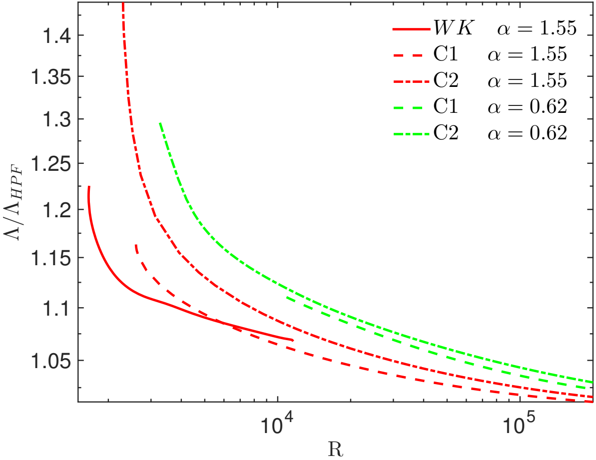


Friction factor ratio $\Lambda/\Lambda_{HPF}$ vs. $R$ for lower branch $WK$, $C1$ and $C2$ solutions at $\alpha = 1.55$, $\alpha = 0.624$; note $\Lambda = \Lambda_{HPF} = 64/R$ for Hagen-Poiseuille flow.

$$\Lambda := \frac{64R}{{R_m}^2}\,, \quad \text{where} \quad R_m := 2\overline{w}R$$

# Rolls

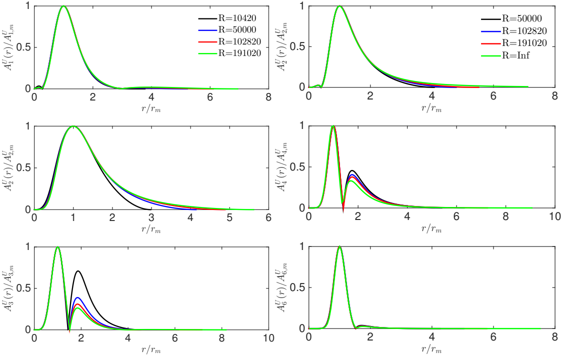


(a) $C1$ (b) $C2$

Scaled radial roll amplitude $A_k^U(r)/A_{k,m}^U$ vs. $r/r_m$. for $k = 2, 4, 6$ for $\alpha = 1.55$. $A_{k,m}^U$ is the maximum roll amplitude attained at $r = r_m$

# Waves

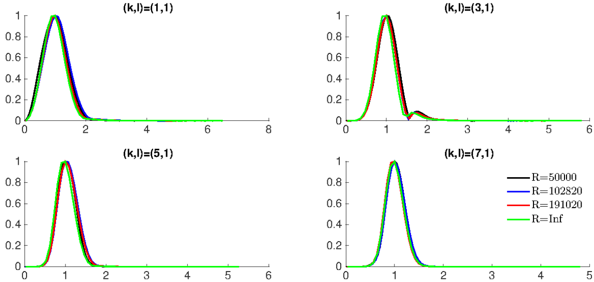


Scaled axial wave amplitude $w_{kl}(r)/w_{k,l,m}$ versus $r/r_m$ for $C2$ solution at $l = 1$ for different $k$ for $\alpha = 1.55$.

# Large R Asymptotics for TWs

Introduce rescaled radial variable $\hat{r}$ so that

$$r = \delta \hat{r}$$

and perturbation velocity $\mathbf{v} = \tilde{w}\hat{\mathbf{z}} + \mathbf{v}_\perp$ in scaled variables

$$\mathbf{v}_\perp = \delta_1 \mathbf{U}(\hat{r}, \theta) + \delta_2 \mathbf{u}(\hat{r}, \theta, z)$$

$$\tilde{w} = \delta_3 W(\hat{r}, \theta) + \delta_4 w(\hat{r}, \theta, z)$$

$$\tilde{p} = \delta_5 P(\hat{r}, \theta) + \delta_6 p(\hat{r}, \theta, z)$$

$$1 - c = \delta_c c_1$$

where $\mathbf{U}$ is the scaled roll, $\mathbf{W}$ is the scaled streak, and $\mathbf{u}, w$ the scaled wave components $\langle \mathbf{u} \rangle = 0, \langle \mathbf{w} \rangle = 0$.

Through elaborate consistency arguments, we concluded $R\delta^4$ either $>> 1$ or strictly order one,

$$\delta_5 = (R\delta)^{-2}\,, \delta_1 = (R\delta)^{-1}\,, \delta_2 = R^{-5/6}\delta^{-1/3}\,, \delta_3 = \delta_c = \delta^2\,, \delta_6 = R^{-5/6}\delta^{8/3}$$

The case $\delta = 1$ is the equivalent of Hall-Sherwin ('10) scalings obtained earlier for channel flows.

For $\delta << 1$, *i.e.* collapsing core, we point out two distinct possibilities

1) $\delta = R^{-1/6}$ - Collapsing Vortex Wave Interacting (VWI) state
2) $\delta = R^{-1/4}$ - Nonlinear Viscous Core(NVC)

# Case1: Vortex Wave Interactions (VWI)

$$\delta_1 = (R\delta)^{-1}\ , \delta_2 = R^{-5/6}\delta^{-1/3}\ , \delta_3 = \delta^2$$
$$\delta_4 = R^{-5/6}\delta^{-4/3}\ , \delta_5 = R^{-2}\delta^2\ , \quad \delta_6 = R^{-5/6}\delta^{8/3}\ , \quad \delta_c = \delta^2$$

1- Small linear $O(R^{-5/6}\delta^{-4/3})$ waves concentrated near a critical layer of width $\delta(R\delta^4)^{-1/3}$

2- drives $O(R^{-1}\delta^{-1})$ rolls through quadratic nonlinear averages (Reynolds stress term),

3- which results in $O(\delta^2)$ streaks, enough to alter the base flow to support neutral stable waves.

# VWI governing equations

Waves $(\mathbf{u}, w)$ satisfy

$$\left(c_1 - \hat{r}^2 + W\right) \partial_z w + \mathbf{u} \cdot \nabla_\perp \left(W - \hat{r}^2\right) = \frac{1}{R\delta^4} \Delta_\perp w \ ,$$

$$\left(c_1 - \hat{r}^2 + W\right) \partial_z \mathbf{u} = -\nabla_\perp p + \frac{1}{R\delta^4} \Delta_\perp \mathbf{u} \ ,$$

$$\nabla_\perp \cdot \mathbf{u} + \frac{\partial w}{\partial z} = 0$$

The viscous terms $\frac{1}{R\delta^4} \Delta_\perp (\mathbf{u}, w)$ are negligible outside $O\left((R\delta^4)^{-1/3}\right)$ critical layer around a critical curve defined by $c_1 - \hat{r}^2 + W = 0$.

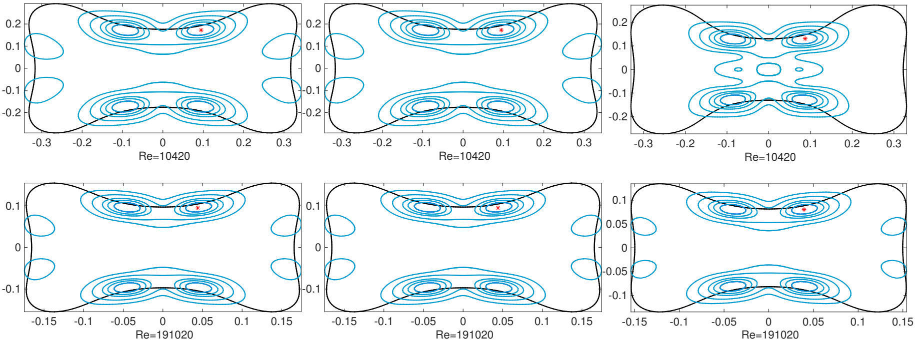


(a) $\alpha = 0.624$ (b) $\alpha = 1.55$ (c) $\alpha = 2.47$

$S_2$ contours for $C1$ solution showing 0.9, 0.8,0.7,0.5 and $0.3\times$ $S_{2,m}$ for three different values of $R$ for given $\alpha$. Critical Curve is shown in black, and location of $S_{2,m}$ shown in $^\circ *$.

Rolls satisfy

$$\mathbf{U} \cdot \nabla_\perp \mathbf{U} = -\nabla_\perp P + \Delta_\perp \mathbf{U} - (R\delta^4)^{1/3} \langle \mathbf{u} \cdot \nabla_\perp \mathbf{u} \rangle - (R\delta^4)^{1/3} \langle w \partial_z \mathbf{u} \rangle \ ,$$

$$\nabla_\perp \cdot \mathbf{U} = 0 \ ,$$

where as $R \to \infty$, the forcing due to waves approaches a delta function supported at the critical curve. To the leading order, the streak is driven only by the rolls as it satisfies

$$\mathbf{U} \cdot \nabla_\perp W = \Delta_\perp W + 2\hat{r} \mathbf{U} \cdot \hat{\mathbf{r}}$$

# Case 2- Nonlinear Viscous Core(NVC): $\delta = R^{-1/4}$

$$\delta_1 = R^{-3/4} = \delta_2 \quad , \quad \delta_3 = R^{-1/2} = \delta_4 \quad , \quad \delta_5 = R^{-3/2} = \delta_6 \, , \quad \delta_c = R^{-1/2}$$

$$\left(c_1 - \hat{r}^2 + \hat{w}\right) \partial_z \hat{\mathbf{v}}_\perp + \hat{\mathbf{v}}_\perp \cdot \nabla_\perp \hat{\mathbf{v}}_\perp = -\nabla_\perp \hat{p} + \Delta_\perp \hat{\mathbf{v}}_\perp$$

$$\left(c_1 - \hat{r}^2 + \hat{w}\right) \partial_z \hat{w} + \hat{\mathbf{v}}_\perp \cdot \nabla_\perp \left(c_1 - \hat{r}^2 + \hat{w}\right) = -H'(z) + \Delta_\perp \hat{w} + \delta^2 \partial_z^2 \hat{w}$$

$$\nabla_\perp \hat{\mathbf{v}}_\perp + \frac{\partial w}{\partial z} = 0$$

for some $2\pi/\alpha$ periodic $H(z)$.

- Recently computed solution to this fully nonlinear eigenvalue problem
- Generally algebraic behavior as $\hat{r} >> 1$.
- Concluded numerical $C1 - C2$ are finite R realization of NVC.
- Similar to Deguchi& Hall (2014) viscous-core solutions in channels.

$(U, V) = \left(\frac{1}{\hat{r}}\psi_\theta, \psi_{\hat{r}}\right)$ where $\psi = \sum_{n=1}^{\infty} \psi_{k_0 n} \sin(k_0 n\theta)$

### Far Field Rolls

$$(U_{4n}, V_{4n}) \sim \hat{r}^{-2n-1} \quad \text{for } n \geq 1 \text{ , for } k_0 = 4$$

$$(U_2, V_2), (U_4, V_4) = O(\hat{r}^{-3}), (U_{2n}, V_{2n}) \sim \hat{r}^{-2n+1} \ln \hat{r} \;\; n \geq 3 \text{ , for } k_0 = 2$$

and $W(\hat{r}, \theta) = \sum_{n=0}^{\infty} W_{k_0 n}(\hat{r}) \cos(k_0 n\theta)$ leads to

### Far-Field Streaks

$$W_0 \sim \hat{r}^{-3}, W_{4n} \sim \hat{r}^{-2n+2} \text{ , for } n \geq 1 \text{ , for } k_0 = 4$$

$$W_0(r) \sim \hat{r}^{-3} \text{ , } W_2 \sim \hat{c}_2, W_4 \sim \hat{c}_4 \text{ , } W_{2n} \sim \hat{r}^{4-2n} \ln \hat{r} \text{ , } n \geq 3 \text{ , for } k_0 = 2$$

Notice there is an azimuthal component of streak that does not go to zero as $\hat{r} \to \infty$, even when rolls, which drive the streak, goes to zero.

Each wave components (u,v,w) represented in the form

$$\sum_{m=0}^{\infty} u_m(\hat{r}, z)\cos(m\theta)$$

satisfy

Far-Field Waves

$$(u_m, v_m) \sim \hat{r}^{-\sqrt{m^2+4}-1}$$

$$w_m \sim \hat{r}^{-\sqrt{m^2+4}-2}$$

# Preliminary findings

- As seen in $c$ vs. $Re$ plot $WK2$ states bifurcate from $WK$ around $Re = 75000$.
- Similar bifurcation observed in $\alpha$ around $\alpha = 3.5$
- Initial finding suggests $WK$ states loose their VWI properties as $\alpha$ increases, higher modes become dominant.
- Linear Stability Analysis on WK2 branch indicate 3 real unstable modes $VWI$ states which scale like, $R^{-1/2}$ ,$R^0$ and $R^{-1}$ similar to Deguchi&Hall '15 observations.
- However, C2 seem to have only one real unstable mode with $R^{-1/2}$ scaling, whereas $C2$ has 2 real unstable both scaling like $Re^{-.5}$. (still need justification)

# Summary

- Found a systematic way to compute traveling wave solutions.
- Asymptotic behaviour was analyzed and connected to numerical calculations.
- We also have partial results of stability. Clearly unstable manifold is low dimensional, suggesting controls that may stabilize these states.
- Since travelling wave solutions have low drag compared to turbulent flow, this may have technological implications.
- Large $R$ number asymptotics important in identifying important mechanisms and interactions.
- Large number $R$ asymptotics of coherent structures equally useful to channel and boundary layer flows.
- Parameter free canonical equations allows us to numerical calculation $R \to \infty$ by computing solutions to parameter free equations.

QUESTIONS?

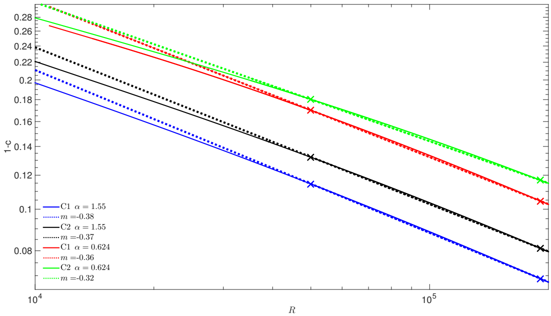


$1 - c$ vs. $R$ in a $\log - \log$ scale for different $\alpha$ for $C1$ and $C2$ solutions. Dotted lines are linear approximations to each curve using larger $R$.

# rolls decay rate $C1$ & $C2$

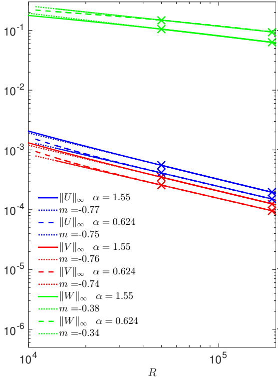


(a) $C1$

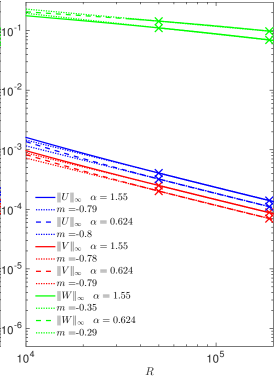


(b) $C2$

Supremum Norm of Roll components $(U, V)$ and of streak $W$ vs. $R$ for $C1$ and $C2$ solution.

# maximal rolls decay rate $C1$

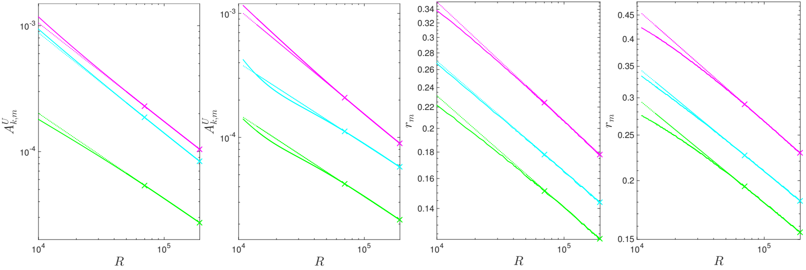


(a) $\alpha = 1.55$ (b) $\alpha = 0.624$ (c) $\alpha = 1.55$ (d) $\alpha = 0.624$

Maximal radial roll amplitude $A^U_{k,m}$ and its location $r_m$ for $k$-th azimuthal component versus $R$ for $C1$ solution for $\alpha = 1.55$ and $\alpha = 0.624$ when $k = 1$ (——), 2 (——), 3 (——). Dotted lines show linear fittings. Negative slopes of dotted lines (from top to bottom) are (a) $0.78, 0.79, 0.67$, (b) $0.84, 0.65, 0.66$, (c) $0.23, 0.21, 0.22$, (d) $0.23, 0.22, 0.22$

# maximal rolls decay rate $C2$

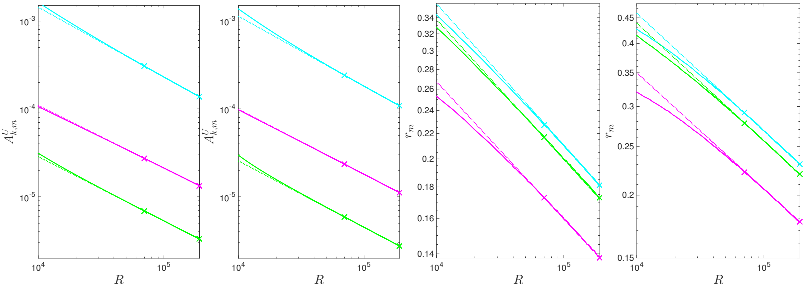


(a) $\alpha = 1.55$ (b) $\alpha = 0.624$ (c) $\alpha = 1.55$ (d) $\alpha = 0.624$

Maximal radial roll amplitude $A^U_{k,m}$ and its location $r_m$ for $k$-th azimuthal component vs $R$ for $C2$ solution for $\alpha = 1.55$ and $\alpha = 0.624$ when $k = 2$ (——), 4 (——), 6 (——). Dotted lines show linear fittings. Negative slopes of dotted lines (from top to bottom) are (a) 0.79, 0.71, 0.73, (b) 0.79, 0.74, 0.75, (c) 0.23, 0.23, 0.22, (d) 0.33, 0.23, 0.23

# maximal streak decay rate $C1$

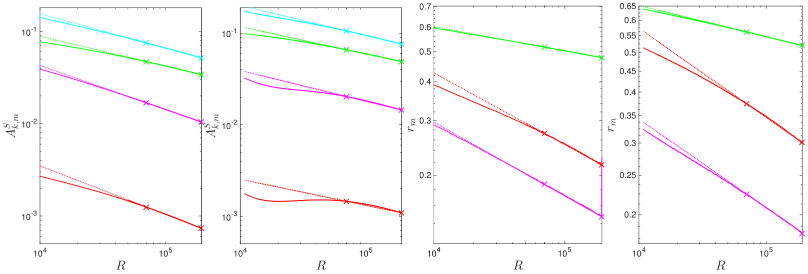


(a) $\alpha = 1.55$ (b) $\alpha = 0.624$ (c) $\alpha = 1.55$ (d) $\alpha = 0.624$

Maximal $k$-th streak amplitude $A^S_{k,m}$ vs. $R$ and its location $r_m$ vs. $R$ for $C1$ solution for $k = 0$(——), 1(——), 2(——), 3(——) for $\alpha = 1.55$ and $\alpha = 0.624$. $k = 0$ is missing in (c),(d) since it has a flat profile. Dotted lines show linear fittings. Negative slopes of dotted lines (from top to bottom) are (a) 0.37, 0.33, 0.47, 0.53, (b) 0.33, 0.29, 0.33, 0.28, (c) 0.07, 0.23, 0.24, (d) 0.07, 0.21, 0.22

# maximal streak decay rate $C2$

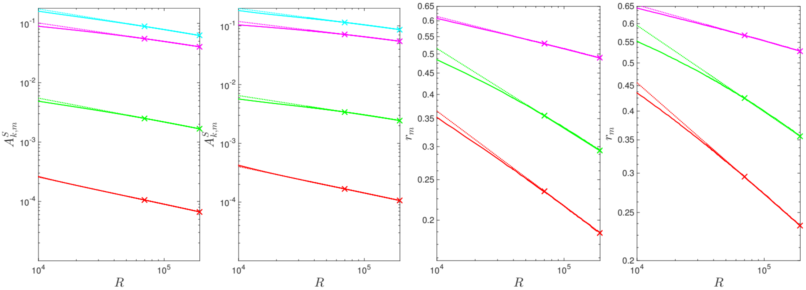


(a) $\alpha = 1.55$ (b) $\alpha = 0.624$ (c) $\alpha = 1.55$ (d) $\alpha = 0.624$

Maximal $k$-th streak amplitude $A^S_{k,m}$ vs. $R$ and and its location $r_m$ vs. $R$ for $C2$ solution for $k = 0$(——), 2(——), 4(——), 6(——) for $\alpha = 1.55$ and $\alpha = 0.624$. $k = 0$ is missing in (c),(d) since it has a flat profile. Dotted lines show linear fittings. Negative slopes of dotted lines (from top to bottom) are (a) 0.35,0.31,0.40, 0.45, (b) 0.28, 0.26, 0.33, 0.45, (c) 0.07, 0.19, 0.23, (d) 0.07, 0.17, 0.22.

## maximal wave decay rate

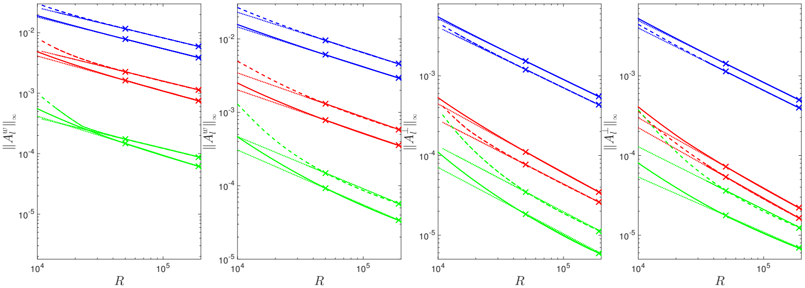


(a) $C1$ (b) $C2$ (c) $C1$ (d) $C2$

Supremum over $(r,\theta)$ of $A_l^w(r,\theta)$ and $A_l^\perp(r,\theta)$ at $l = 1$(——/- - -), 2(——/- - -), 3(——/- - -) for $C1$ and $C2$ solutions for different $\alpha$. Solid lines correspond to $\alpha = 1.55$, while dashed lines represent $\alpha = 0.624$. Dotted lines show linear fittings. Negative slopes of dotted lines (from top to bottom) are (a) $0.50, 0.52, 0.51, 0.58, 0.50, 0.65$, (b) $0.54, 0.54, 0.60, 0.59, 0.71, 0.70$, (c) $0.76, 0.76, 0.86, 0.80, 0.84, 0.83$, (d)$0.78, 0.78, 0.88, 0.88, 0.69, 0.78$.

# Supplementary Materials:Symmetries

Rotational $k_0$-fold symmetry in azimuthal direction $\theta$ by

$$R_{k_0} : (u, v, w, p)(r, \theta, z) \to (u, v, w, p)(r, \theta + 2\pi/k_0, z)$$

$S_1$ Rotate and Reflect symmetry:

$$S_1 : \quad (r, \theta, z) \to (-r, \theta + \pi, z) \quad \textit{implies} \quad (u, v, w, p) \to (-u, -v, w, p)$$

Shift -and -Reflect symmetry $S$ on a $z$-periodic pipe is introduced as

$$S : (u, v, w, p)(r, \theta, z) \to (u, -v, w, p)(r, -\theta, z + \pi/\alpha),$$

leaves equations invariant. So the solution $\boldsymbol{v}$ is either $S$-symmetric ($S - even$) or $S$-antisymmetric ($S - odd$) i.e.

$$S - even : (r, \theta, z) \to (r, -\theta, z{+}\pi/\alpha) \quad \textit{implies} \quad (u, v, w, p) \to (u, -v, w, p)$$

$$S - odd : (r, \theta, z) \to (r, -\theta, z{+}\pi/\alpha) \quad \textit{implies} \quad (u, v, w, p) \to (-u, v, w, p).$$

# NSE in Cylindrical Component Form

When $\boldsymbol{v} = (u, v, w)$ and $\vec{v}_B = (u^B, v^B, w^B)$, the equation becomes,

$$-c\frac{\partial u}{\partial z} = -\frac{\partial q}{\partial r} + \frac{1}{R}\Delta u - \frac{2}{r^2}\frac{\partial v}{\partial \theta} - \frac{u}{r^2} - (\vec{v}_B \cdot \nabla)u + \frac{2v^B v}{r} - (\boldsymbol{v} \cdot \nabla)u^B$$

$$-c\frac{\partial v}{\partial z} = -\frac{1}{r}\frac{\partial q}{\partial \theta} + \frac{1}{R}\Delta v + \frac{2}{r^2}\frac{\partial u}{\partial \theta} - \frac{v}{r^2} - (\vec{v}_B \cdot \nabla)v - \frac{2v^B v}{r} - (\boldsymbol{v} \cdot \nabla)v^B$$

$$-c\frac{\partial w}{\partial z} = -\frac{\partial q}{\partial z} + \frac{1}{R}\Delta w - (\vec{v}_B \cdot \nabla)w - (\boldsymbol{v} \cdot \nabla)w^B$$

$$u(1, \theta, z) = v(1, \theta, z) = w(1, \theta, z) = 0$$

where operators are defined as

$$(\vec{v}_B \cdot \nabla) = u^B\frac{\partial}{\partial r} + \frac{v^B}{r}\frac{\partial}{\partial \theta} + w^B\frac{\partial}{\partial z}, \qquad (\boldsymbol{v} \cdot \nabla) = u\frac{\partial}{\partial r} + \frac{v}{r}\frac{\partial}{\partial \theta}$$

$$\Delta = \frac{\partial^2}{\partial r^2} + \frac{1}{r}\frac{\partial}{\partial r} + \frac{1}{r^2}\frac{\partial^2}{\partial \theta^2} + \frac{\partial^2}{\partial z^2}$$

# Numerical Formulation: Computation of Vortex-Wave states

- Galerkin in $\theta$ and $\tilde{z}$ direction, Collocation in $r$ with $r_j = \cos\dfrac{(2j+1)\pi}{4N}$, $0 \le j \le N$ .

$$\Phi_j(r;k) = \begin{cases} T_{2j+2}(r) - T_{2j}(r) & k \text{ odd} \\ T_{2j+3}(r) - T_{2j+1}(r) & k \text{ even} \end{cases}$$

for $u_{kl}(r)$ and $v_{kl}(r)$, and

$$\Psi_j(r;k) = \begin{cases} T_{2j+3}(r) - T_{2j+1}(r) & k \text{ odd} \\ T_{2j+2}(r) - T_{2j}(r) & k \text{ even} \end{cases}$$

for $w_{kl}(r)$.

The resulting nonlinear algebraic equation is solved using Newton's Method. The solution process has three important elements:

i) Elimination of pressure from the equation to reduce the number of unknown variables.

ii) Efficiently solving the linear system $\boldsymbol{J}(\vec{X})\delta\vec{X} = -F(\vec{X})$ at each Newton Step (for matrices of size $10000 \times 10000$).

# i) Pressure Elimination

Instead of solving for divergence equation in the NSE, pressure term is eliminated:

$$\Delta q = \mathcal{N}(\boldsymbol{v}) \tag{2a}$$

where $\mathcal{N}$ is a nonlinear operator acting on $\boldsymbol{v}$, complemented with Neumann boundary conditions

$$\frac{\partial q}{\partial r} = \mathcal{N}_b(\boldsymbol{v}) \tag{2b}$$

Resulting Poisson equation is solved using pseudospectral techniques in $\theta$ and $\tilde{z}$ to compute $\mathcal{N}(\boldsymbol{v})$, then invert $\Delta$ efficiently at the discrete $r$ values. We denote $\mathcal{L} = \Delta^{-1}$ with Neumann B.C. (2b) and replace $\nabla q$ in VW equation by $\nabla \mathcal{L}(\mathcal{N}(\boldsymbol{v}))$.

# ii) Newton's Method - Jacobian Matrix

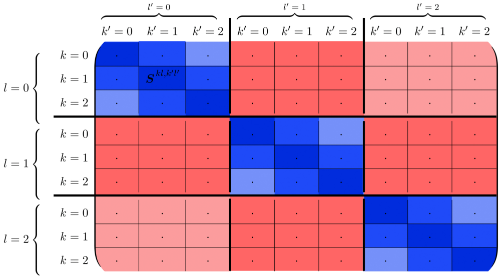


Block structure of the Jacobian Matrix when $M=2$ and $P=2$.

Velocity scalings suggest that Jacobian blocks get smaller as we move away from the big diagonal.

$$\underbrace{\frac{1}{R}\Delta \boldsymbol{v} + c\frac{\partial \boldsymbol{v}}{\partial z}}_{\textbf{Linear-1}} - \underbrace{((\vec{v}_B\cdot\nabla)\boldsymbol{v} + (\boldsymbol{v}\cdot\nabla)\vec{v}_B)}_{\textbf{Linear-2}} - \underbrace{(\nabla\mathcal{L}(\mathcal{N}(\boldsymbol{v})) + (\boldsymbol{v}\cdot\nabla)\boldsymbol{v})}_{\textbf{Nonlinear}} = 0$$

# ii) Newton's Method - Iterative Method

Due to large number of unknowns for the velocity $\boldsymbol{v}$, we need to use GMRES iterative method to solve the matrix equation at each Newton's Step. Assuming we have a good initial guess, a preconditioner is chosen in the form

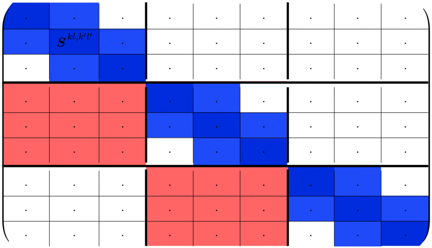


Preconditioner matrix $\mathcal{M}$ for $M = 2, P = 2$.

using scaling properties of the NSE.

# Initial Guess Procedure via Suction, $s \neq 0$

Results from linear stability analysis of the base flow $\vec{v}_B$ when $s = 10$

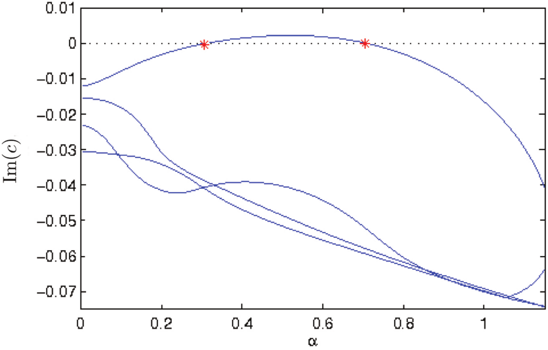


$\alpha$ vs. Im($c$). Linear Stability of the 4 least stable eigenvector $\boldsymbol{v}$'s.

# Roll Asymptotics

Axial averaging $\langle \cdot \rangle$ of NSE, the projection in orthogonal plane results in

$$\delta^{-1}\delta_1^2 \mathbf{U}\cdot\nabla_\perp \mathbf{U} = -\delta_5\delta^{-1}\nabla_\perp P + \delta_1\delta^{-2}R^{-1}\Delta_\perp \mathbf{U} - \delta^{-1}\delta_2^2\langle \mathbf{u}\cdot\nabla_\perp \mathbf{u}\rangle - \delta_4\delta_2\langle w\frac{\partial}{\partial z}\mathbf{u}$$

$$\nabla_\perp \cdot \mathbf{U} = 0$$

- divergence condition requires $P$ appeara in the leading order asymptotics $\delta_5 = \delta_1^2$.
- involve viscous term must be present for steady nontrivial solution $\delta_1\delta = R^{-1}$.

# Full Equations

Axial averaging results in

$$\left(c_1 - \frac{\delta^2}{\delta_3}\hat{r}^2 + W + \frac{\delta_2}{\delta\delta_3}w\right)\partial_z w + \frac{1}{R\delta^2\delta_3}\left(\mathbf{U}\cdot\nabla_\perp\right)w$$

$$+\frac{\delta_2}{\delta\delta_3}\mathbf{u}\cdot\nabla_\perp w + \mathbf{u}\cdot\nabla_\perp\left(W - \frac{\delta^2}{\delta_3}\hat{r}^2\right)$$

$$= -\delta^2\frac{\partial p}{\partial z} + \frac{1}{R\delta^2\delta_3}\Delta_\perp w + \frac{1}{R\delta_3}\partial_z^2 w + \frac{\delta_2}{\delta\delta_3}\langle\mathbf{u}\cdot\nabla_\perp w\rangle$$

$$\left(c_1 - \frac{\delta^2}{\delta_3}\hat{r}^2 + W + \frac{\delta_2}{\delta\delta_3}w\right)\partial_z\mathbf{u} + \frac{1}{R\delta^2\delta_3}\left(\mathbf{U}\cdot\nabla_\perp\right)\mathbf{u} + \frac{1}{R\delta^2\delta_3}\left(\mathbf{u}\cdot\nabla_\perp\right)\mathbf{U}$$

$$+\frac{\delta_2}{\delta\delta_3}\mathbf{u}\cdot\nabla_\perp\mathbf{u} = -\nabla_\perp p + \frac{1}{R\delta^2\delta_3}\Delta_\perp\mathbf{u} + \frac{1}{R\delta_3}\partial_z^2\mathbf{u} + \frac{\delta_2}{\delta\delta_3}\langle\mathbf{u}\cdot\nabla_\perp\mathbf{u}\rangle + \frac{\delta_2}{\delta\delta_3}\langle w\partial_z\mathbf{u}\rangle\,,$$

$$\nabla_\perp\cdot\mathbf{u} + \frac{\partial w}{\partial z} = 0$$

# NVC-Canonical Equation

transforms into the following set of scaled nonlinear equations

$$\left(c_1 - \hat{r}^2 + \hat{w}\right) \partial_z \hat{\mathbf{v}}_\perp + \hat{\mathbf{v}}_\perp \cdot \nabla_\perp \hat{\mathbf{v}}_\perp = -\nabla_\perp \hat{p} + \Delta_\perp \hat{\mathbf{v}}_\perp + \delta^2 \partial_z^2 \hat{\mathbf{v}}_\perp \tag{3}$$

$$\left(c_1 - \hat{r}^2 + \hat{w}\right) \partial_z \hat{w} + \hat{\mathbf{v}}_\perp \cdot \nabla_\perp \left(c_1 - \hat{r}^2 + \hat{w}\right) = -\delta^2 \partial_z \hat{p} + \Delta_\perp \hat{w} + \delta^2 \partial_z^2 \hat{w} \tag{4}$$

$$\nabla_\perp \cdot \hat{\mathbf{v}}_\perp + \frac{\partial \hat{w}}{\partial z} = 0 \tag{5}$$

To the leading order, $\delta^2 = O(R^{-1/2})$